

Supplementary Information

Interleukin-13 receptor $\alpha 2$ is a novel marker and potential therapeutic target for human melanoma

Hayato Okamoto¹, Yasuhiro Yoshimatsu^{1,2}, Taishi Tomizawa¹, Akiko Kunita³, Rina Takayama², Teppei Morikawa³, Daisuke Komura⁴, Kazuki Takahashi², Tsukasa Oshima⁵, Moegi Sato¹, Mao Komai¹, Katarzyna A. Podyma-Inoue², Hiroaki Uchida^{1,6}, Hirofumi Hamada¹, Katsuhito Fujiu^{5,7}, Shumpei Ishikawa⁴, Masashi Fukayama³, Takeshi Fukuhara^{1,8} and Tetsuro Watabe^{1,2}

¹Laboratory of Oncology, School of Life Sciences, Tokyo University of Pharmacy and Life Sciences, Tokyo, Japan,

²Department of Biochemistry, Graduate School of Medical and Dental Sciences, Tokyo Medical and Dental University (TMDU), Tokyo, Japan,

³Department of Pathology, Graduate School of Medicine, The University of Tokyo, Tokyo, Japan,

⁴Department of Genomic Pathology, Medical Research Institute, Tokyo Medical and Dental University (TMDU), Tokyo, Japan,

⁵Department of Cardiovascular Medicine, Graduate School of Medicine, The University of Tokyo, Tokyo, Japan,

⁶Project Division of Cancer Biomolecular Therapy, The Institute of Medical Science, The University of Tokyo, Tokyo, Japan,

⁷Department of Advanced Cardiology, Graduate School of Medicine, The University of Tokyo, Tokyo, Japan,

⁸Department of Neurology, Juntendo University School of Medicine, Tokyo, Japan

Materials and methods

Gene expression analysis of publicly available data

RNA-sequencing data of *IL13RA2* from the Cancer Cell Line Encyclopedia (CCLE) project were downloaded from the Broad CCLE portal and 1444 cell lines were used for the analysis. RNA-sequencing data of the Cancer Genome Atlas (TCGA) for skin cutaneous melanoma (SKCM) were obtained from Firehose using the Bioconductor package RTCGAToolbox (version 2.8.0). A provisional dataset of 469 samples were used for the analysis. Spearman rank correlation was used to assess correlation between gene expression levels.

Figure legends

Figure S1. *In silico* analysis of *IL13RA2* expression. Cancer Cell Line Encyclopedia (CCLE) was used to study the frequency of *IL13RA2* expression in various types of carcinoma cell lines.

Figure S2. Immunohistochemical analysis for IL13R α 2 expression in A375, A375-IL13RA2 KO, or A2058 xenograft and normal human tissues. (A) A375 xenograft (B) A375-IL13RA2 KO xenograft (C) A2058 xenograft, (D) testis, (E) stomach, (F) pancreas, (G) kidney, (H) lung. Scale bars: 50 μ m.

Figure S3. Effect of IL-13 on the *in vitro* proliferation of various melanoma cells. In all, (A) 8×10^4 of SK-MEL-28, (B) 8×10^4 of SK-IL13R α 2 and (C) 1.8×10^4 of A375 cells, were seeded into 6-well plates and were grown in the presence or absence of IL-13. The cells were harvested after (A) 2, (B) 2 or (C) 3 days, respectively, and were counted. The number of cells at the indicated time period are expressed as mean \pm SD. * $p < 0.05$; Student's t-test.

Figure S4. Effect of IL13R α 2 expression on tumour angiogenesis. Sections of tumours derived from the SK-MEL-28 ($n = 6$) and SK-IL13R α 2 ($n = 5$) cells were subjected to immunofluorescence staining with the anti-PECAM-1 antibody. Scale bar: 100 μ m.

Figure S5. Correlation between *IL13RA2* and *AREG* mRNA expression levels in melanoma tissues. A scatter plot revealing the correlation between the *IL13RA2* mRNA and *AREG* mRNA expressions.

Figure S6. Effect of IL13R α 2 on VEGF expression in various melanoma cells. (A) The SK-MEL-28 melanoma cells were transfected with the IL13R α 2 expression vector, followed by qRT-PCR analysis to determine the expression of IL13R α 2 (top) and VEGF (bottom). (B) *IL13RA2* was knocked out in the A375 melanoma cells, followed by qRT-PCR analysis for the expression of IL13R α 2 (top) and VEGF (bottom). All values are mean \pm SD. * $p < 0.05$; Student's t-test.

Figure S7. Full-length blots of cropped images shown in Figure 5A.

Supplementary Table 1. Summary of tissue microarray

Slide name	Position	Ratio of IL13RA2+ cells (%)	Organ	Pathological diagnosis
ME1004e	A10	10	Skin	Malignant melanoma of right sole
ME1004e	B2	15	Skin	Malignant melanoma of sole
ME1004e	C7	2	Skin	Malignant melanoma of heel
ME1004e	D8	90	Skin	Malignant melanoma of left thigh
ME1004e	D9	40	Vulva	Malignant melanoma of cunnus
ME1004e	H1	10	Lymph node	Metastatic malignant melanoma from armpit
ME1004e	E1	3	Skin	Malignant melanoma
ME1004e	E5	15	Skin	Malignant melanoma
ME1004e	F8	5	Skin	Malignant melanoma
ME1004e	G3	3	Skin	Malignant melanoma
ME1004e	A7	1	Skin	Malignant melanoma
ME208	D2	1	Skin	Malignant melanoma of left chest wall
ME208	D6	2	Skin	Malignant melanoma
ME208	H4	1	Lymph node	Metastatic malignant melanoma from armpit

Supplementary Table 2. Primers for quantitative RT-PCR

Transcript	Primer	Sequence (5' to 3')
<i>GAPDH</i> (GAPDH)	5'	GAAGGTGAAGGTCGGAGTC
	3'	GAAGATGGTGATGGGATTTC
<i>ACTB</i> (β -actin)	5'	TCACCCACACTGTGCCCATCTACGA
	3'	CAGCGGAACCGCTCATTGCCAATGG
<i>IL13RA2</i> (IL13R α 2)	5'	TAAACCTTTGCCGCCAGTCT
	3'	AGGTCCCAAAGGTATGCTCC
<i>AREG</i> (amphiregulin)	5'	GTGTCCCAGAGACCGAGTTG
	3'	ATGGTTCACGCTTCCCAGAG
<i>VEGFA</i> (VEGF-A)	5'	AGGCCAGCACATAGGAGAGA
	3'	TTTCTTGCGCTTTCGTTTTT

Fig. S1

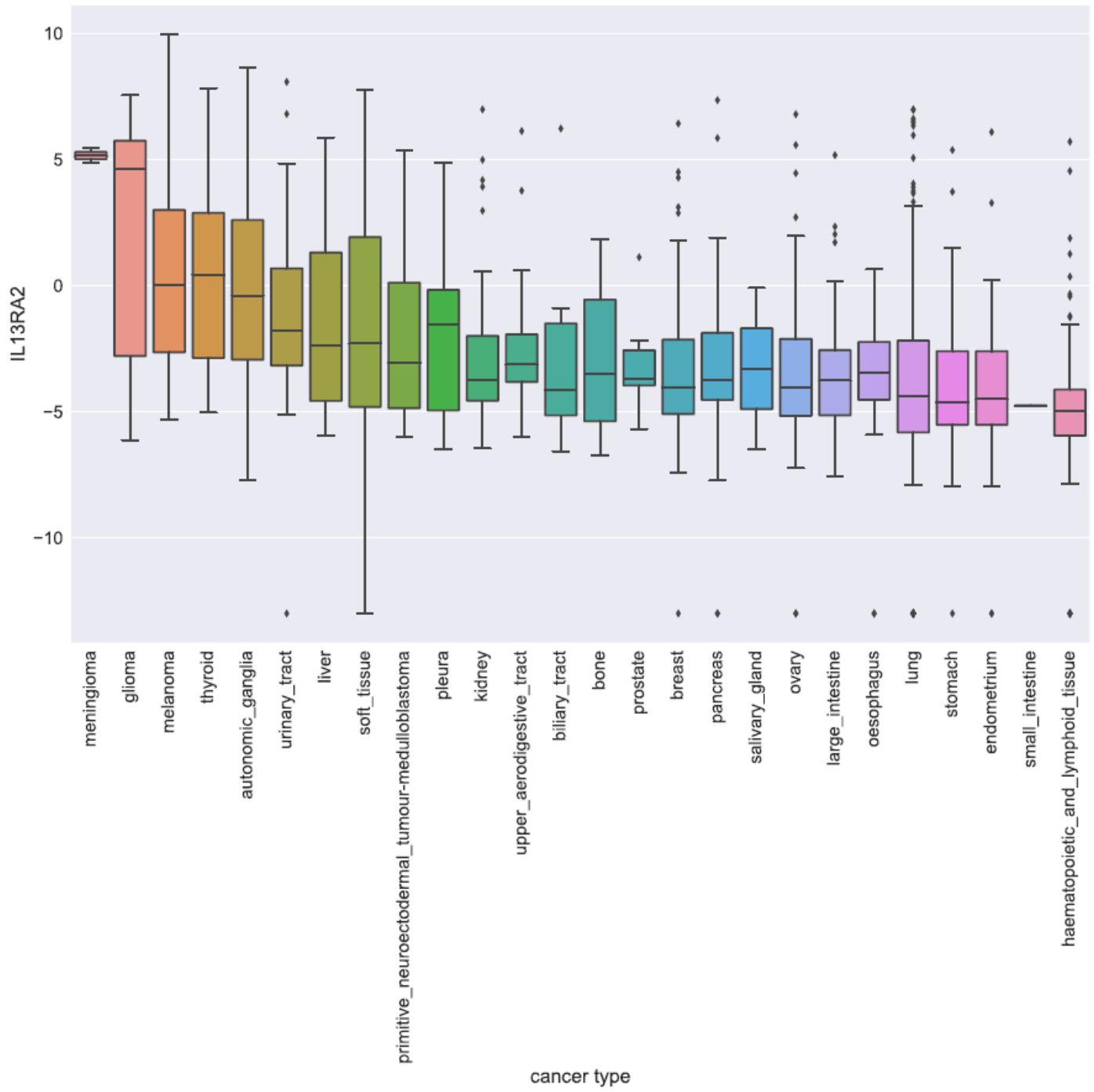


Fig. S2

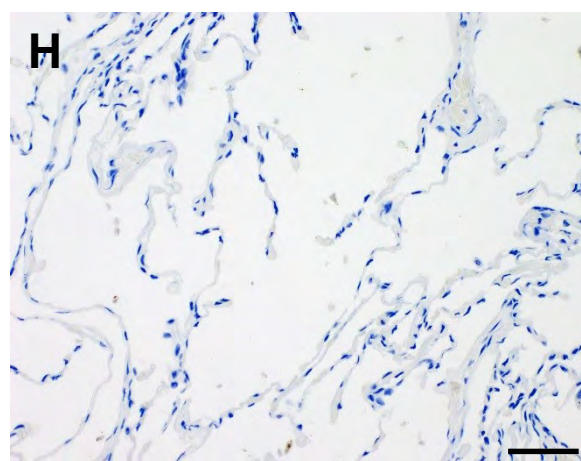
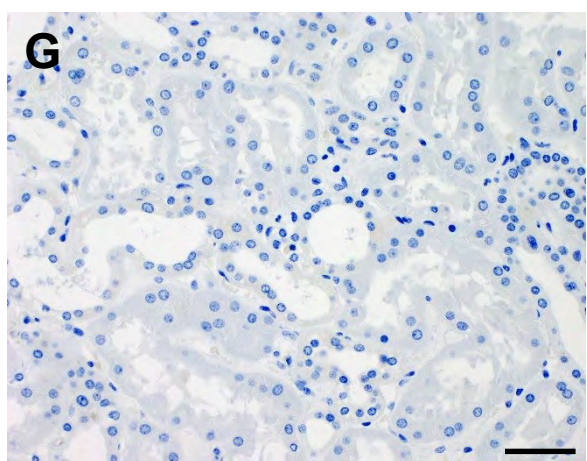
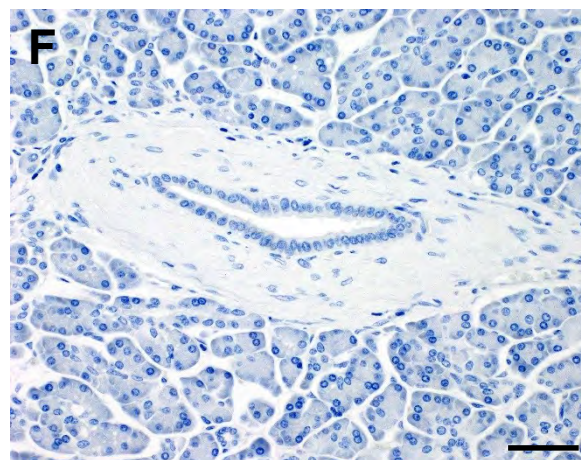
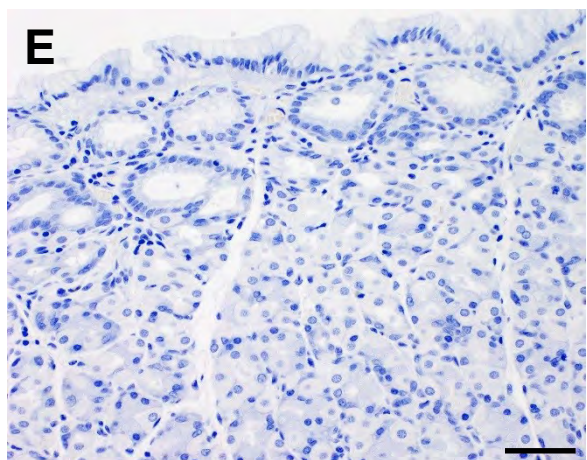
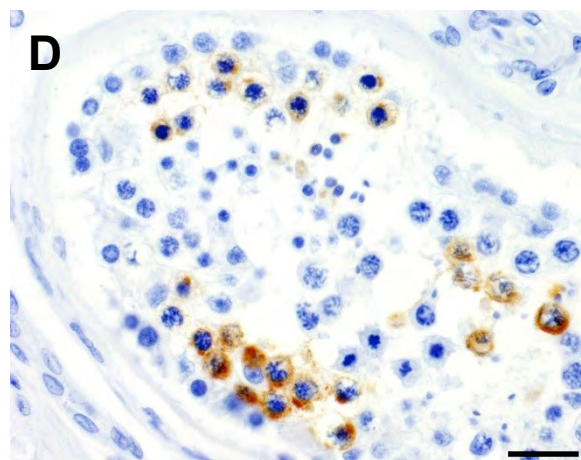
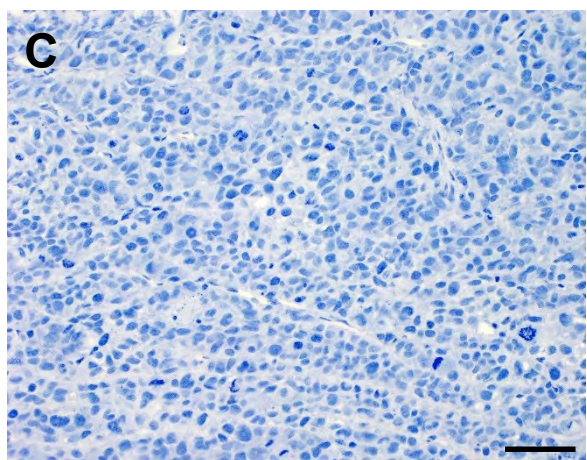
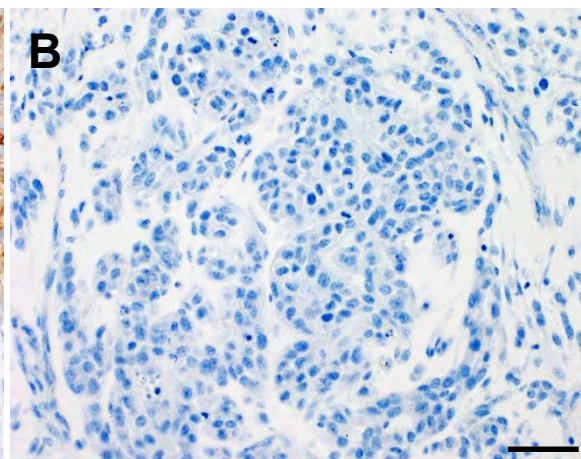
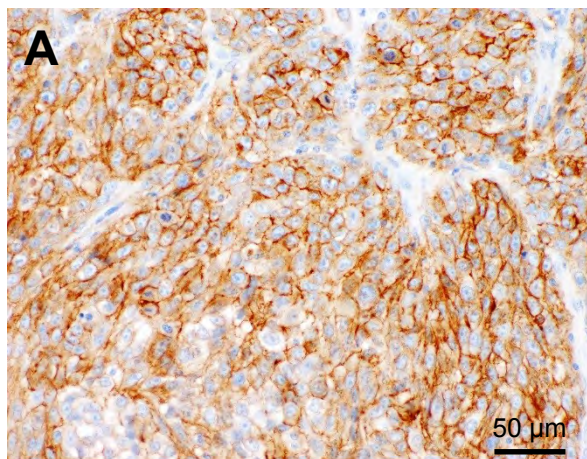
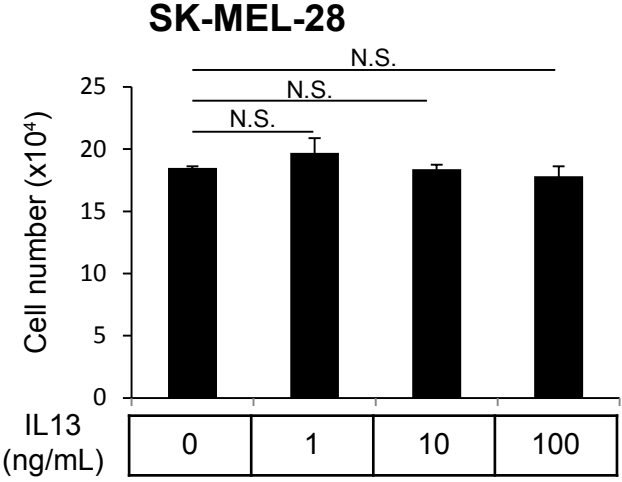
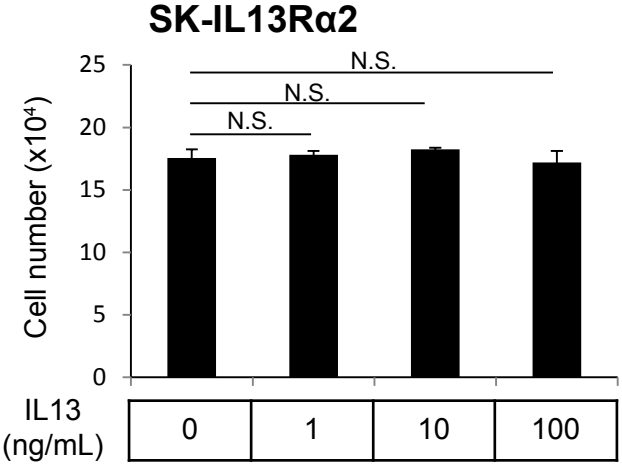


Fig. S3

A



B



C

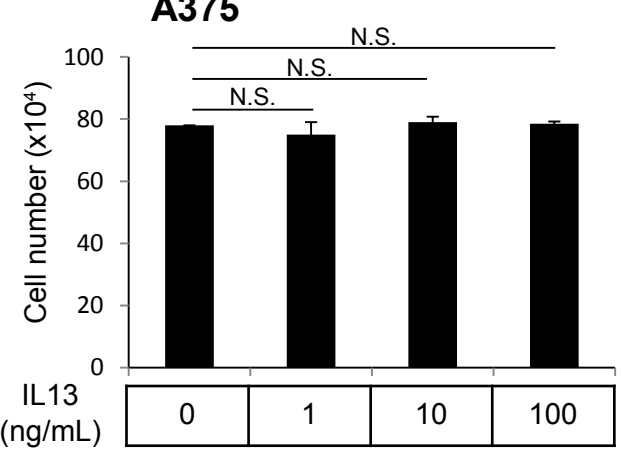


Fig. S4

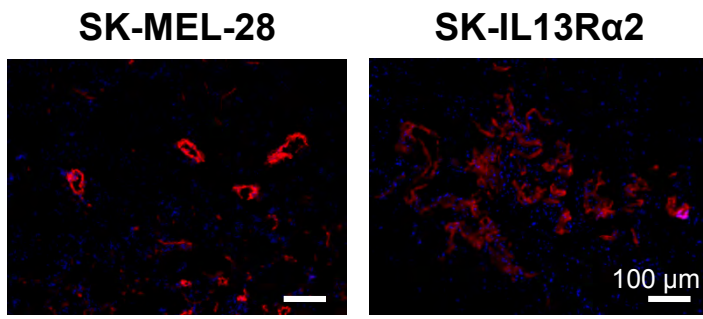


Fig. S5

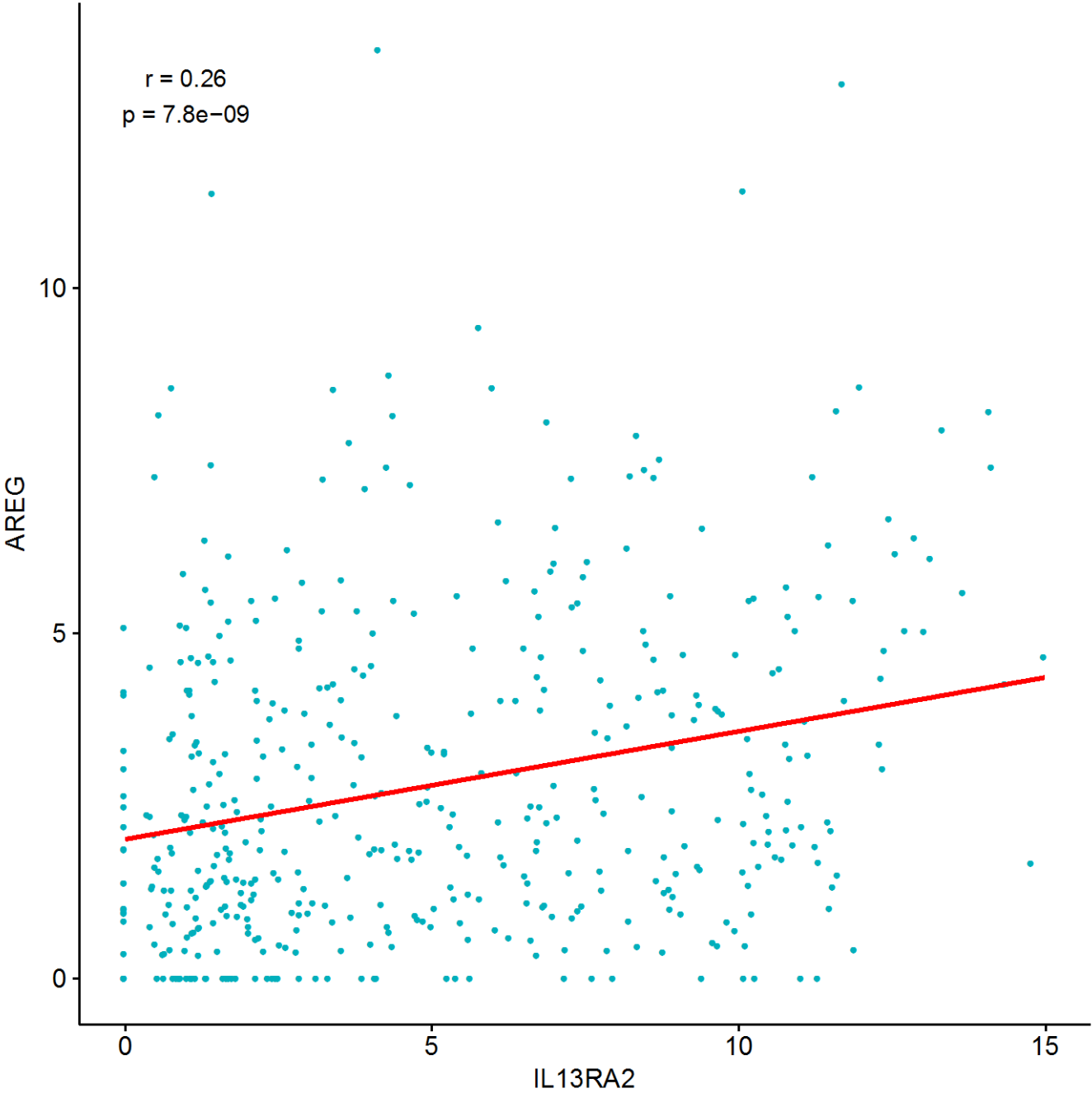


Fig. S6

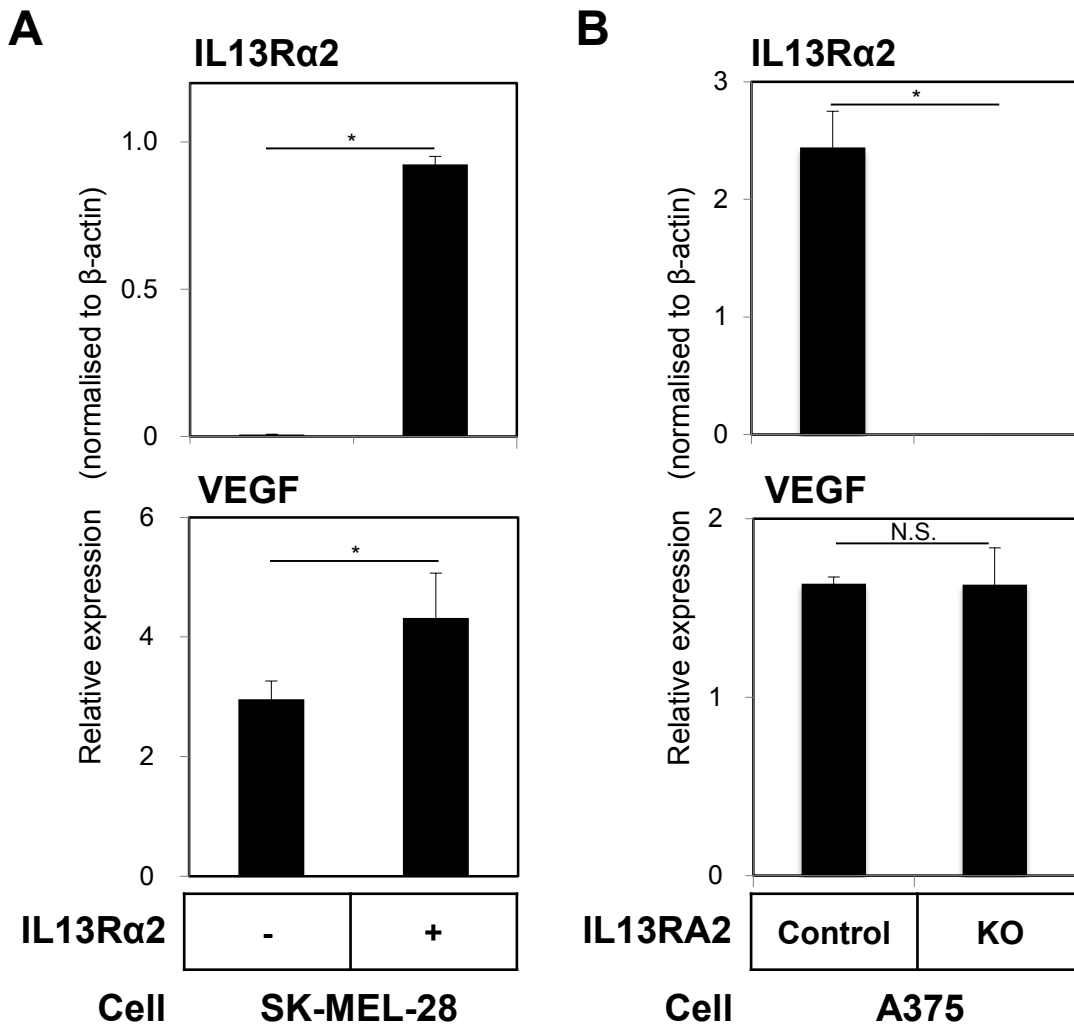
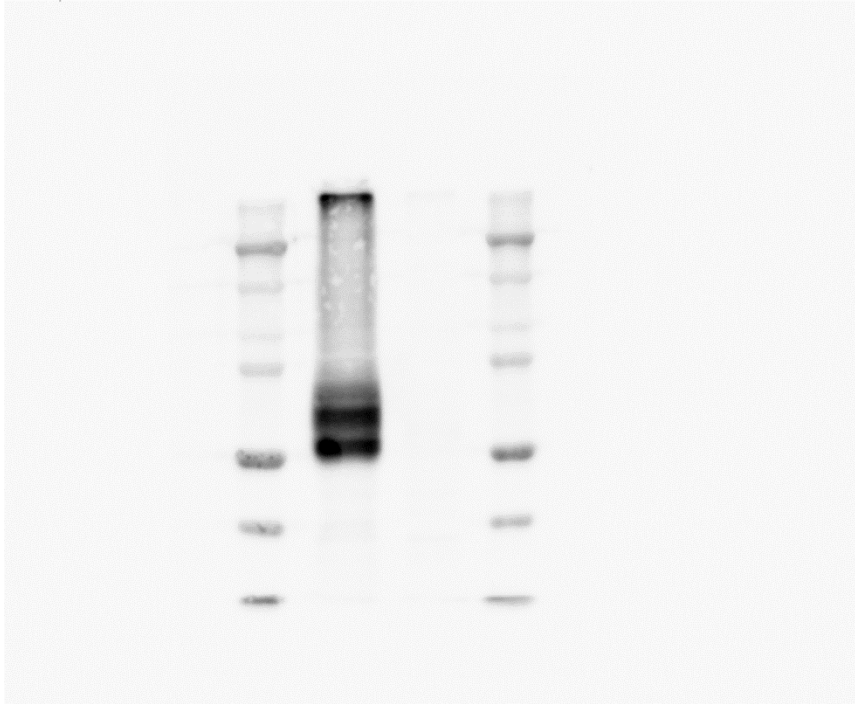


Fig. S7

IL13R α 2



β -actin

